RECONFIGURABLE DUAL REFLECTOR FOR A REALISTIC MISSION SCENARIO IN KU BAND

C. Cappellin, K. Pontoppidan, H-H. Viskum

TICRA, Læderstræde 34, 1201 Copenhagen, Denmark, Email: ticra@ticra.com

INTRODUCTION

The possibility of employing the same spacecraft at several orbital locations, changing the coverage region, and compensating for varying weather conditions are the main reasons why reconfigurable antennas for contoured beam generation can provide significant advantages in satellite communications. Though extremely attractive in terms of cost and manufacturing, shaped reflectors lack so far the capability of being reconfigured in orbit, while this feature can be obtained by an array-fed parabolic reflector.

Several examples of possible reconfigurable shaped reflectors were studied over the years [1]-[4]. Today the most promising technology is constituted by a mesh of interwoven flexible wires with circular cross section which is supported by a number of control points and has a free rim [4]. While the mathematical properties of the model and an application to two simple coverages with a single offset shaped reflector can be found in [4], we study here the use of a reconfigurable shaped dual reflector in a realistic mission scenario in Ku band. In particular we will focus on the advantages in terms of performances that a mechanically reconfigurable subreflector together with a fixed shaped main reflector can provide. Reflectors will be optimized with the traditional spline shaping while the mesh of interwoven flexible wires, which is meant to be applied to the subreflector, will be considered in a following study.

INTERCONTINENTAL MISSION SCENARIO

The scenario under investigation is the so-called Intercontinental mission suggested by Thales Alenia Space (TAS). It is constituted by three coverages, one over Central Africa, one over South Africa and one over Russia, see Fig. 1. The coverages are illuminated by a geostationary satellite which can be located between 10E and 70E. The gain required over the coverages is given in Table 1. A minimum XPD of 30 dB and a beam pointing error of 0.12° shall be considered, while no isolation constraints are expected. The antenna shall work in Tx/Rx case in the frequency bands Tx=10.95-12.50 GHz and Rx=13.75-14.5 GHz.

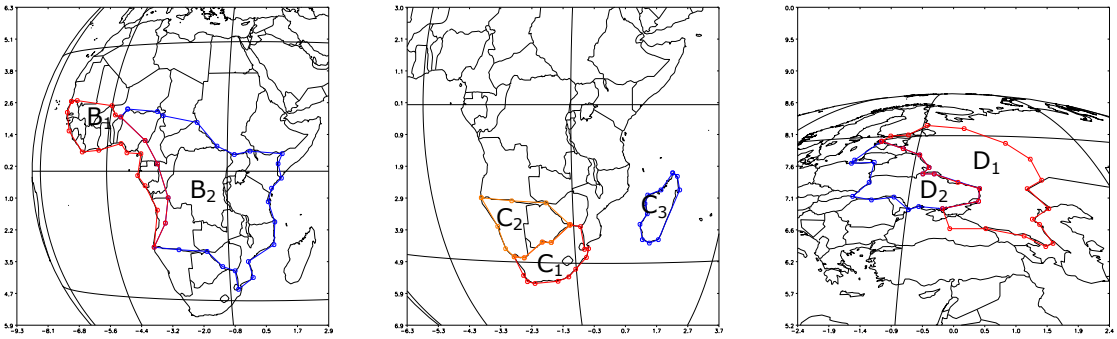

Figure 1. Polygons B_1, B_2, C_1, C_2 and C_3 and D_1 and D_2 seen from 36E.

In general, reconfigurability is foreseen 18 times in the satellite life time (approximately once a year) and is required both in varying the satellite orbital location and in switching from one coverage to the other.

Table 1. Gain requirements for the coverages B_1+B_2, C_1+C_2+C_3 and D_1+D_2.

Polygon and antenna gain		Polygon and antenna gain		Polygon and antenna gain	
B_1	Ref	C_1	Ref	D_1	Ref
B_2	Ref - 4 dB	C_2	Ref - 1 dB	D_2	Ref - 4 dB
		C_3	Ref - 7 dB		

ANTENNA OPTICAL SYSTEM

A dual offset Gregorian reflector antenna mounted on the spacecraft lateral side generates all coverages. The main reflector consists of a paraboloid in the *xyz*-coordinate system (CS), with circular projected aperture of diameter D = 2.4 m, focal length f = 2.4 m and clearance d' = 0.3 m, see Fig. 2. The subreflector is an ellipsoid with circular projected aperture D_2 = 0.8 m. The Mizuguchi condition is applied.

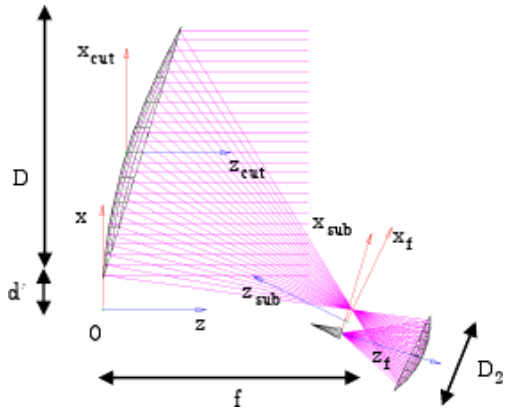

Figure 2. Dual reflector geometry and coordinate systems definition.

The feed is linearly polarized along x_f and y_f, where $x_f\, y_f\, z_f$ is the feed CS, with origin at the second focal point of the ellipsoid, z_f pointing towards the center of the subreflector and x_f lying on the *xz*-plane. Far-fields results which will be given in the following are expressed in the cut CS $x_{cut}\ y_{cut}\ z_{cut,}$ which is parallel to the *xyz*-CS and with origin at the center point of the reflector surface.

OPTIMIZATION RESULTS

With the purpose of limiting the number of optimizations but at the same time investigating the largest number of parameters, a single orbital location (36E) is considered. Five frequencies (10.95, 11.7, 12.5, 13.75 and 14.5 GHz) and only one polarization (x_f) of the feed are taken into account. First, the satellite CS $x_s\, y_s\, z_s$ is defined, with origin at the satellite location, x_s-axis towards West, y_s-axis towards North and z_s-axis pointing towards the center of the Earth. It coincides with the cut CS of the antenna. The three coverages are then written in the satellite CS and the approximate center of each coverage (u_i,v_i) with i = 1, 2, 3 is identified. The antenna can only provide service to one coverage at the time. The entire antenna, once mounted on the satellite, points towards the approximate center of gravity of all the coverages denoted by (u_g,v_g). While the feed and the subreflector are fixed in this position, the main reflector is equipped with a reflector pointing mechanism (RPM) by which it is tilted towards the midpoint between (u_g,v_g) and (u_i,v_i), depending on the coverage the antenna has to generate. In the following, the achieved directivity levels at f =12.5 GHz will be shown. A RPM will be assumed in every test case.

Shaped subreflector and shaped main reflector for each individual coverage

In order to evaluate the advantages and limitations provided by a reconfigurable subreflector, the results given by a non reconfigurable main reflector and subreflector, both shaped for each individual coverage, will first be shown. This constitutes the best possible design for a shaped but fixed dual reflector optimized for each individual coverage. The main reflector and subreflector surfaces were shaped with the software POS5 [5] with the well-established spline modeling in order to satisfy the requirements on gain and XPD on each individual coverage. On each coverage, 30 splines and 12 splines were chosen to shape the main reflector and the subreflector respectively, on the basis of the convergence mechanism and the size of the main reflector. The minimum directivity obtained over the coverages is given in Table 2 while the amplitude of the co-polar component of the obtained far-fields together with the polygons in the satellite CS are shown in Fig. 3. It is seen that contour levels agree very well with the desired regions and that obviously a higher directivity can be obtained over the smaller coverages.

Table 2. Directivity obtained for the coverages B_1+B_2, C_1+C_2+C_3 and D_1+D_2 with 30 splines for the main reflector and 12 splines for the subreflector on each individual coverage.

Polygon and antenna gain		Polygon and antenna gain		Polygon and antenna gain	
B_1	30.9 dB	C_1	34.5 dB	D_1	36.1 dB
B_2	26.9 dB	C_2	33.5 dB	D_2	32.1 dB
		C_3	27.5 dB		

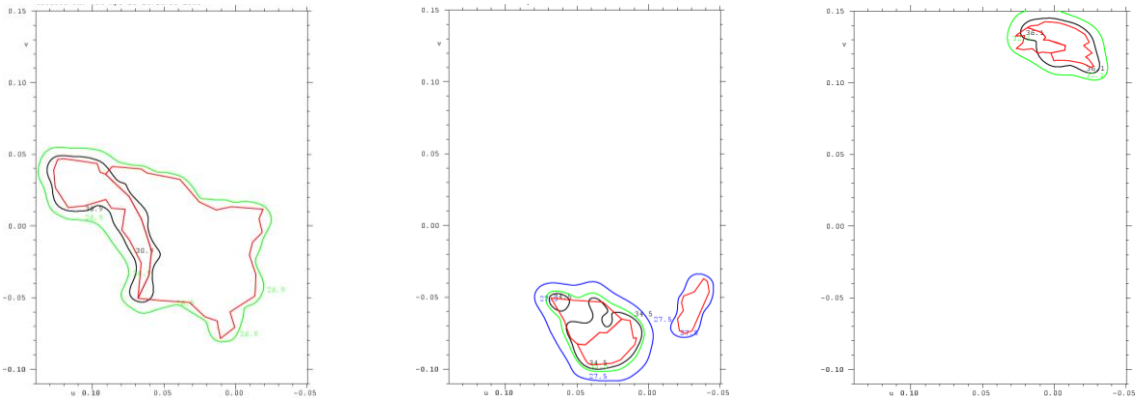

Figure 3. Coverage polygons (red curve) and amplitude of the co-polar component (minimum levels) of the obtained far-field in dBi in the satellite CS.

Ellipsoidal subreflector and shaped fixed main reflector

The performances of a traditional fixed main reflector shaped to maximise at the same time the minimum directivity on all the coverages was then analyzed. This represents the best and only possible solution when reconfigurability of the antenna cannot be achieved. Again, 30 splines were chosen to shape the main reflector, while the subreflector was kept ellipsoidal. The new directivity levels obtained over the coverage regions are given in Table 3, while the contour plots of the amplitude of the co-polar component of the obtained far-fields are shown in Fig. 4. It is seen that 2.9 dB over B_1+B_2, 4 dB over C_1+C_2+C_3 and 4.1 dB over D_1+D_2 are lost with respect to optimum case of Table 2.

Table 3. Directivity obtained for the coverages B_1+B_2, C_1+C_2+C_3 and D_1+D_2 with 30 splines for the fixed main reflector and an ellipsoidal subreflector.

Polygon and antenna gain		Polygon and antenna gain		Polygon and antenna gain	
B_1	28 dB	C_1	30.5 dB	D_1	32 dB
B_2	24 dB	C_2	29.5 dB	D_2	28 dB
		C_3	23.5 dB		

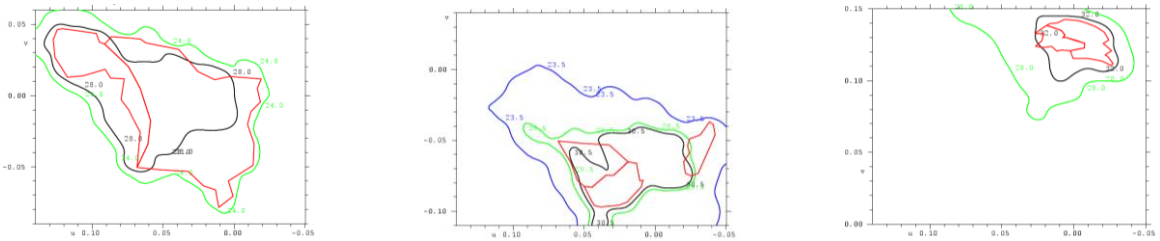

Figure 4. Coverage polygons (red curve) and amplitude of the co-polar component (minimum levels) of the obtained far-field in dBi in the satellite CS.

Reconfigurable subreflector and shaped fixed main reflector

The results given by a shaped but fixed main reflector and a reconfigurable subreflector, optimized for each individual coverage, are finally discussed. The obtained directivity levels are reported in Table 4 and the amplitude of the co-polar component of the far-fields is shown in Fig. 5. Again, 30 splines and 12 splines were used to shape the main and subreflector respectively. It is observed that this antenna configuration improves the directivity levels over all the

coverages by 2.7 dB with respect to Table 3. At the same time, the obtained directivities differ from the optimum levels of Table 2 by 0.2 dB over B_1+B_2, 1.3 dB over $C_1+C_2+C_3$, and 1.4 over D_1+D_2. In this sense, the possibility of reconfiguring the subreflector shape for every coverage constitutes a very good improvement in respect of the traditional technology given by a shaped but fixed main reflector with RPM.

Table 4. Directivity obtained for the coverages B_1+B_2, $C_1+C_2+C_3$ and D_1+D_2 with 30 splines for the fixed main reflector and 12 splines for the reconfigurable subreflector.

Polygon and antenna gain		Polygon and antenna gain		Polygon and antenna gain	
B_1	30.7 dB	C_1	33.2 dB	D_1	34.7 dB
B_2	26.7 dB	C_2	32.2 dB	D_2	30.7 dB
		C_3	26.2 dB		

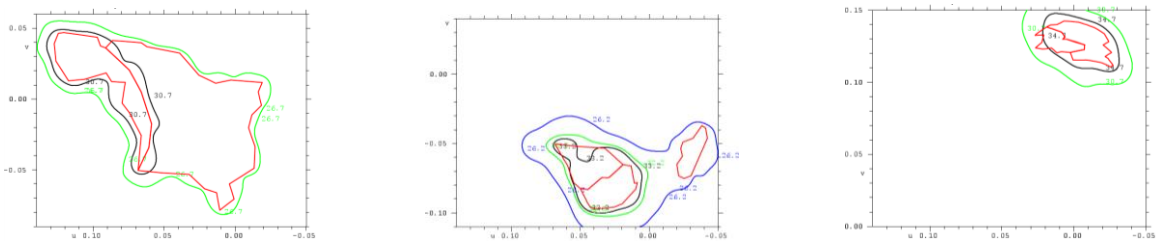

Figure 5. Coverage polygons (red curve) and amplitude of the co-polar component (minimum levels) of the obtained far-field in dBi in the satellite CS.

The shape of the fixed main reflector was then computed relative to the initial paraboloid in the cut CS and it was found that the *z*-values of the surface were in the range of [0 cm:6 cm], with the majority of the values contained in the interval [0 cm:3 cm]. The *z*-coordinates of the subreflector shapes, in the subreflector CS depicted in Fig. 2, were then computed relative to the initial ellipsoid. In Fig. 6 the subreflector spline shaping used to illuminate the region $C_1+C_2+C_3$ is shown on the left in cm scale, while the difference with respect to the subreflector surface used to illuminate B_1+B_2 is shown on the right. It is seen that the deviation of the shaped reconfigurable subreflector is in the range of [-7 mm:7 mm].

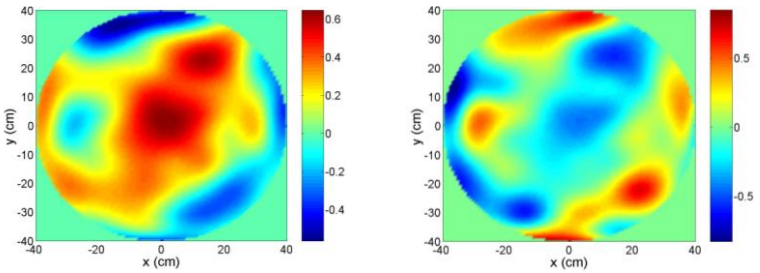

Figure 6. Spline shaped subreflector surface in cm relative to the parent ellipsoid: on the left the subreflector to illuminate $C_1+C_2+C_3$, on the right the difference with the one used to illuminate B_1+B_2.

REFERENCES

[1] K. Pontoppidan, "Reconfigurable reflector surfaces with imparted bending stiffness," *TICRA report S-582-02*, September 1994.

[2] R. C. Brown, P. J. B. Clarricoats, Z. I. Hai, "The performance of a prototype reconfigurable mesh reflector for spacecraft antenna applications," *Proceedings of the 19th European Microwave Conference*, September 1999.

[3] L. Datashvili, H. Baier, J. Schimitschek, M. Huber, "High precision large deployable space reflector based on pillow-effect-free technology," *Proceedings of the 48th Structures, Structural Dynamics and Materials Conference*, Honolulu, Hawaii, USA, May 2007.

[4] K. Pontoppidan, "Light weight reconformable reflector antenna dish," Proceedings of the 28th ESA Antenna Workshop on Space Antenna Systems and Technologies, Noordwijk, The Netherlands, June 2005.

[5] Homepage of POS5, http://www.ticra.com/script/site/page.asp?artid=6&cat_id=38, April 2008.